arXiv:astro-ph/0101218v1 13 Jan 2001

Measuring Feedback in Damped Lyα Systems

Arthur M. Wolfe

University of California, La Jolla CA 92093-0424, USA

Abstract. We measure feedback (heating rates) in damped Lyα systems (DLAs) from the cooling rate of the neutral gas. Since cooling occurs through [C II] 158 μm emission, we infer cooling from C II* 1335.7 absorption lines detected with HIRES on the Keck I telescope. The inferred heating rates are 30 times lower than for the Galaxy ISM. At $z \approx 2.8$ the implied star formation rate per unit area is $\log\psi_*=-2.4\pm0.3$ $M_\odot$ y^{-1} kpc^{-2} and the star formation rate per unit comoving volume $\log d\rho_*/dt=-0.8\pm0.2 M_\odot$ y^{-1} Mpc^{-3}. This is the first measurement of star formation rates in objects that typify the protogalactic mass distribution.

1 Introduction

The purpose of this paper is to discuss a new method for probing physical conditions in DLAs. In principle, this technique can be used to probe their masses, sizes, and baryonic content. The focus of this paper is on star formation. Specifically, in this paper I infer the star formation rates per unit area in DLAs by measuring the rate at which the *neutral* gas is heated. This is possible because it is reasonable to attribute heating to far UV radiation emitted by massive stars. Since the cross-sectional area times the comoving density of the DLAs is known, we can derive the rate of star formation per unit comoving volume. Until now, comoving star formation rates have been obtained for highly luminous objects such as the Lyman Break Galaxies. Here I derive comoving star formation rates for objects that are more representative of the protogalactic mass distribution.

2 [C II] 158 μm Emission From Damped Lyα Systems

[C II] 158 μm emission results from transitions between the $^2P_{3/2}$ and $^2P_{1/2}$ fine-structure states in the ground term of C$^+$. It dominates the cooling rate by the Galaxy ISM with a luminosity $L([\text{C II}]) = 5\times10^7 L_\odot$ [1]. Most of the emission from the Galaxy and other nearby spirals arises in the diffuse neutral gas rather than from star-forming regions in spiral arms, or PDRs on the surfaces of molecular clouds (e.g. [2]). The last point is especially relevant for DLAs where molecules are rarely detected [3].

In order to estimate the [C II] 158 μm emission rates, Pottasch et al. [4] derived the following expression for the 158 μm luminosity per H atom:

$$l_c = N(\text{CII}^*) h\nu_{ul} A_{ul} / N(\text{HI}) \text{ erg s}^{-1} \text{ H}^{-1} \quad , \tag{1}$$

where N(C II*) is the column density of C$^+$ ions in the $^2P_{3/2}$ state, N(H I) is the H I column density, and A_{ul} and $h\nu_{ul}$ are the Einstein A coefficient and energy of the $^2P_{3/2} \rightarrow {}^2P_{1/2}$ transition. In fact, l_c is the density−weighted average along the sightline of $l_{cr}(\mathbf{r})$, the emission rate per H atom at a given displacement vector $\mathbf{r}$. Here $l_{cr}(\mathbf{r}) = n_{\rm CII^*}(\mathbf{r})A_{ul}h\nu_{ul}/n_{\rm HI}(\mathbf{r})$, where $n_{\rm CII^*}$ and $n_{\rm HI}$ are the volume densities of H I and C II* .

Figure 1 shows estimates of l_c versus N(H I), where N(C II*) is deduced from the strength of C II* 1335.708 absorption and N(H I) from DLA absorption. The small stars depict measurements for several sightlines through the ISM [4] and [5]. The large star depicts $< l_c >$, i.e., $l_{cr}(\mathbf{r})$ averaged over the H I disk of the Galaxy. Figure 1 also shows our measurements of l_c for 27 DLAs. As neither 158 μm nor 21 cm emission has been detected from any DLAs, $< l_c >$ cannot be inferred directly, where in this case $< l_c >$ corresponds to $l_{cr}(\mathbf{r})$ integrated over the volume of the average DLA. Nevertheless, comparison between the two distributions of l_c clearly indicates $< l_c >$ for the DLAs to be a factor of 30 or more lower than for the ISM.

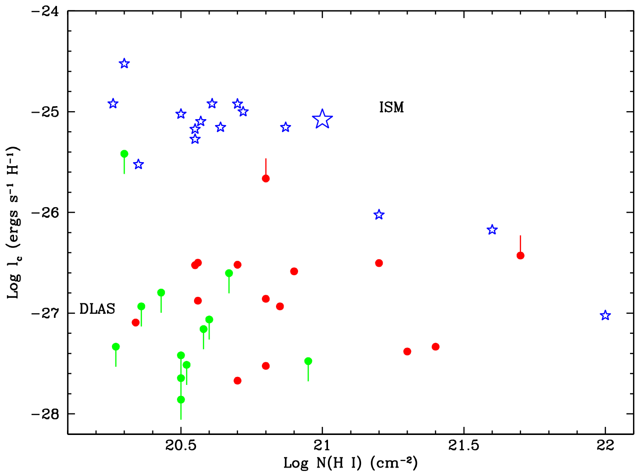

Fig. 1. l_c versus N(H I) for DLAs (solid circles) and sightlines through the ISM (stars). Upper limits are 2-σ. Large star is $< l_c > = L$([C II])/($m_H M$(H I)) where L([C II]) and M(H I) are the 158 μm luminosity and H I mass of the Galaxy.

3 PROPERTIES OF MULTI-PHASE MEDIA

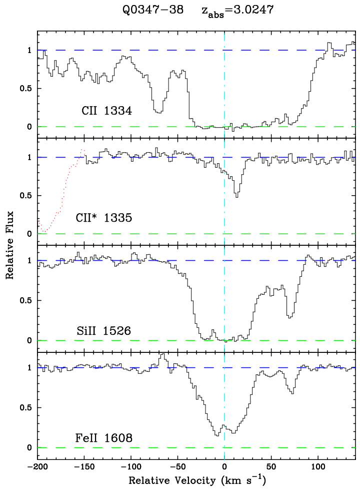

Fig. 2. Keck HIRES absorption profiles for C II* 1335.7 and 3 resonance lines in the z = 3.0247 damped absorber toward Q0347−348. Comparison between the C II* and unsaturated Fe II 1608 profiles shows evidence for a CNM at v = + 10 km s^{-1} and WNM at − 10 km s^{-1}

To determine the heating rate from measurements of l_c we consider the thermal and ionization equilibria of gas subjected to heating and cooling. The result is a multi-phase medium in which the various phases are in pressure equilibrium. There are indications that the H I gas in DLAs is in two phases: a cold ($T \geq 50$ K) neutral medium (CNM), and a warm ($T \sim 8000$K) neutral medium (WNM). The detection of 21 cm absorption in DLAs indicates the presence of a CNM since the 21 cm optical depth is inversely proportional to temperature [6]. Evidence for a WNM comes from misalignment in velocity space between 21 cm absorption or C II* 1335.7 absorption on the one hand and UV resonance lines on the other (see Figure 2), since the CNM dominates 158 μm emission (Fig. 3c).

To compute the properties of the multi-phase gas we focus on the thermal and ionization balance of the atomic CNM and WNM. By analogy with the ISM we assume that heating is dominated by photoelectric ejection of electrons from grains illuminated by far UV radiation ($h\nu$=8→13.6 eV). We adopt the formalism of [7] who considered small grains and PAHs and found the photoelectric heating rate at $\mathbf{r}$ to be given by

$$\mathit{\Gamma}_d(\mathbf{r}) = 1.0{\times}10^{-24}\epsilon G_0(\mathbf{r}) \ \mathrm{ergs\ s^{-1}\ H^{-1}} \quad . \qquad (2)$$

In the last equation $G_0(\mathbf{r})$, the radiation field incident at $\mathbf{r}$, equals $4\pi J(\mathbf{r})$ and is in units of Habing's [8] estimate of the local interstellar value (=1.6×10^{-3} ergs cm^{-2} s^{-1}). Here J is the mean intensity integrated between 8 and 13.6 eV, and ϵ is the far-UV heating efficiency. Following [7] we include ionization and heating by cosmic rays and assume that the dust-to-gas ratio equals the metallicity, $Z/Z_{\odot}$. As a result $\Gamma_d(\mathbf{r})$ is proportional to $Z/Z_{\odot}$.

An example of the computed 2-phase diagrams is shown in Figure 3. Here we assume $G_0 = 1.7$ which corresponds to the far UV radiation field in the ISM (see [7]). We also let the cosmic ray ionization rate $\zeta = 1.8\times10^{-17}\ s^{-1}$ (see [7]). For comparisons with the DLA data we let [Fe/H] ($\equiv \log Z/Z_{\odot}$) $= -1.5$, the mean metallicity of the DLAs ([9]). Since regions of thermal stability occur where $\partial(\log P)/\partial(\log n) > 0$, a stable 2-phase medium, comprising the WNM and CNM, can exist between the local pressure minimum and maximum. Figure 3c shows that $l_{cr}(\mathbf{r})$ asymptotically approaches a maximum at log $n > 1.5$ cm^{-3} in the CNM where it dominates the cooling rate. Comparison with Figure 1 further indicates that this $l_{cr}(\mathbf{r})$ is much lower than the $< l_c >$ observed in the ISM, but falls within the range of l_c spanned by the DLAs.

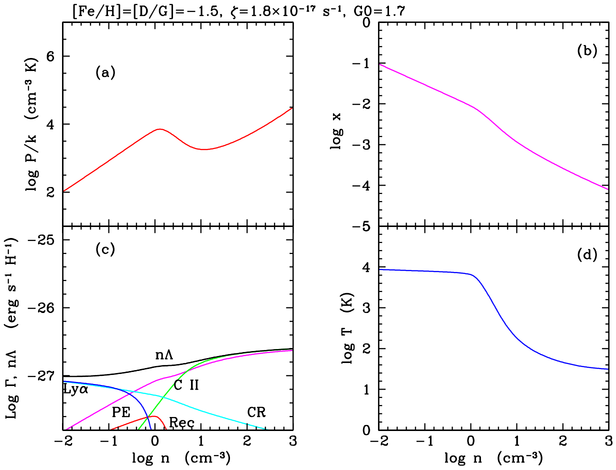

Fig. 3. (a)Pressure vs. H density, n. (b) Electron fraction vs. n. (c) Photoelectric (PE) and cosmic-ray (CR) heating rates vs. n. Lyα , [C II] (i.e., $l_{cr}(\mathbf{r})$), grain recombination (Rec), and total ($n\Lambda$) cooling rates vs. n. (d) Temperature vs. n.

4 Star Formation Rates

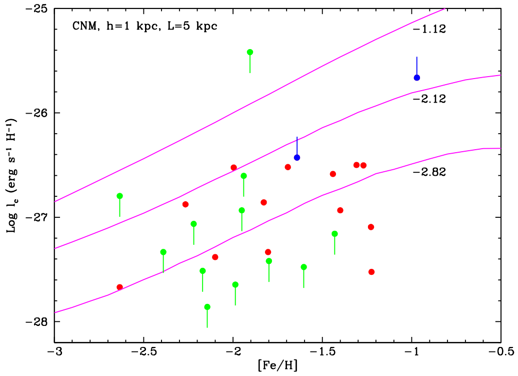

Fig. 4. Computed $l_{cr}(\mathbf{r})$ vs. [Fe/H] for $\log\psi_* =$ -2.8,-2.1, and -1.1 $M_\odot y^{-1} kpc^{-2}$. Data for DLAs show l_c versus [Fe/H].

The previous discussion suggests that the far UV radiation field in high-z DLAs is similar to that in the Galaxy. Because the far UV intensity is proportional to the rate at which massive stars form [10], the star formation rates should be likewise similar. More precisely, the similarity is between the star formation rates per unit area, since solutions to the radiative transfer equation for plane parallel slabs of dust and stars show that J_ν is proportional to the luminosity per unit area, μ_ν [11]. Here we compute J_ν at the center of a uniform slab of stars and dust, and then integrate solutions for J_ν to J with [11]'s fit to the far UV spectrum of the ISM radiation field. Finally we combine J with eq. (2) to compute the heating rates.

The curves in Figure 4 plot the resultant $l_{cr}(\mathbf{r})$ versus [Fe/H]. The $l_{cr}(\mathbf{r})$ are computed in the CNM limit, $l_{cr}(\mathbf{r})=\mathit{\Gamma}_d(\mathbf{r})$, and for $\mathbf{r}$ corresponding to the central points of uniform slabs. The curves are parameterized by 3 different values of ψ_*, the star formation rate per unit area. Comparison with the DLA data reveals significant variations of l_c at fixed [Fe/H]. This indicates that ψ_* is distributed at constant metallicity. The data also show tentative evidence for the predicted decrease in $l_{cr}(\mathbf{r})$ with decreasing [Fe/H] at an apparent upper limit to the star formation rate of $\log\psi_* \approx -2.12\ M_\odot \mathrm{y}^{-1}\mathrm{kpc}^{-2}$. However, we cannot rule out entirely a possibility currently under investigation; namely, that the DLA sightlines pass through gas containing only WNM [12] in which case the ψ_* in Figure 4 are lower limits.

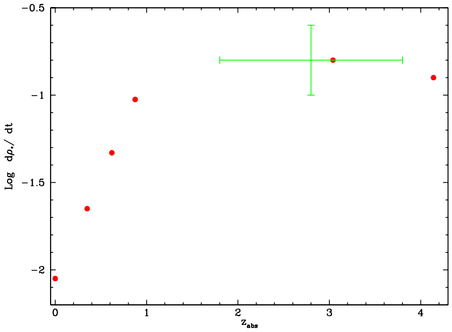

Fig. 5. Star formation rates per unit comoving volume computed for $\Omega_m = 1$,$\Omega_\Lambda = 0$,h=0.5 cosmology. Circles denote luminous galaxies [14] and point with error bars, DLAs. Horizontal error bar depicts redshift range of DLA sample.

The star formation rate per unit comoving volume is given by

$$d\rho_*/dt = \frac{<\psi_*> (A/A_p) \times dN/dz}{(1+z)^3(-cdt/dz)} \quad . \tag{3}$$

where $<\psi_*>$ is the average star formation rate per unit area, A and A_p are the average cross-sectional area and cross-sectional area projected on the sky, and dN/dz is the number of DLAs per unit redshift interval. Assuming log$<\psi_*> = -2.4 \pm 0.3$ $M_\odot$ y^{-1} kpc^{-2} and dN/dz=0.24 at $z = 2.8$ [13], the median redshift of our sample, we find that in the plane-parallel limit (i.e., $A = 2A_p$), log$d\rho_*/dt = -0.8 \pm 0.2$ $M_\odot y^{-1} Mpc^{-3}$. This result, plotted in Figure 5, is compared with estimates derived from objects detected in emission such as the Lyman Break galaxies [14]. It is encouraging that the DLA measurement is not widely different from measurements made with independent techniques. The similarity could mean that the DLAs and Lyman Break galaxies are the same entity. More likely, our estimates of ψ_* and $d\rho_*/dt$ suggest the DLAs to be characterized by low specific star formation rates and high comoving densities relative to the Lyman Break galaxies.

Acknowledgements: I wish to thank C. F. Mckee and J. X. Prochaska for many valuable comments. This research was partially supported by NSF grant AST0071257.

References

1. Wright, E. L. et al. 1991 Preliminary Spectral observations of the galaxy with a $7'$ beam by the cosmic background explorer (COBE), Ap. J., **381**, 200–209

2. Madden, S. C. et al. 1993 158 micron [C II] mapping of NGC 6946: probing the atomic medium, Ap. J., **407**, 579–587
3. Lu, L., Sargent, W. L. W., & Barlow, T. A. (1998), Abundances of Heavy elements and CO molecules in high redshift damped Lyα Galaxies, in Highly Redshifted Radio Lines, ASP Conf. Ser. 156, eds. C. L. Carilli et al., 132–137 243–250.
4. Pottasch, S. R., Wesselius, P. R., & van Duinen, R. J. (1979) Determination of cooling rates in the interstellar medium, A&A, **74**, L15–L17
5. Gry, C., Lequeux, J., & Boulanger, F. (1992) Fine structure lines of C^+ and N^+ in the galaxy A&A, **266**, 457–462
6. Chengalur, J. N., & Kanekar, N. 2000, Implications of 21 cm observations for damped Lyα systems, astro-ph/00115401
7. Wolfire et al. (1995) The neutral atomic phases of the interstellar medium, Ap. J., **443**, 152–168
8. Habing, H. J. (1968) The interstellar radiation density between 912 Å and 2400 Å, Bull. Astr. Inst. Neth. **19**, 421–431
9. Prochaska, J. X. & Wolfe, A. M. (2000) Metallicity evolution in the early universe ApJ, **533**, L5–L8
10. Madau, P., Pozzetti, L., & Dickinson, M. (1998) The star formation history of field galaxies ApJ, **498**, 106–116
11. Draine, B. T. (1978) Photoelectric heating of the interstellar gas ApJS, **35**, 595–619
12. Norman, C. A. & Spaans, M. (1997) Molecules at high redshift: the evolution of the cool phase of protogalactic disks Ap. J., **480**, 145–154
13. Storrie-Lombardi L., & Wolfe, A. M. (2000) Surveys for $z > 3$ Damped Lyα Absorption Systems: The Evolution of the Neutral Gas. Ap. J., **543**, 552–576
14. Pettini, M. (2000) Private communication